

The Kinetics of Shear-Induced Boundary Film Formation from Dimethyl Disulfide on Copper

Brendan Miller · Octavio Furlong ·
Wilfred T. Tysoe

Received: 3 July 2012 / Accepted: 9 September 2012 / Published online: 19 September 2012
© Springer Science+Business Media, LLC 2012

Abstract The kinetics of the shear-induced surface-to-bulk transport of methyl thiolate species formed from dimethyl disulfide (DMDS) on a copper surface are explored. It is found that the loss of surface species as a function of the number of rubbing cycles can be modeled by assuming that the adsorbed layer penetrates the subsurface a distance of ~ 0.7 nm per scan. Adding wear to this model does not improve the fit to the experimental data providing an upper limit for the wear rate of ~ 0.06 nm/scan. This model is applied to analyzing the depth distribution of sulfur within the subsurface region as a function of the number of rubbing cycles, measured by Auger depth profiling when continually dosing the copper sample with DMDS. It is found that the shape of the experimental depth profile is in agreement with the model developed to analyze the surface-to-bulk transport kinetics of the adsorbed layer. However, the profiles are almost identical for surfaces that have been rubbed 130 and 360 times, so that the surface-to-bulk transport kinetics are self limiting.

Keywords Dialkyl sulfides · Copper · Shear-induced surface-bulk transport kinetics · Auger spectroscopy

B. Miller · W. T. Tysoe (✉)
Department of Chemistry and Laboratory for Surface Studies,
University of Wisconsin-Milwaukee, Milwaukee, WI 53211,
USA
e-mail: wtt@uwm.edu

O. Furlong
INFAP/CONICET, Universidad Nacional de San Luis,
Ejercito de Los Andes 950, 5700 San Luis, Argentina

1 Introduction

It has been found that interfacial shear while rubbing against copper produces nanocrystalline structures in the subsurface region [1–7]. It has also been demonstrated that adsorbed thiolate species on copper, formed by exposing the surface to dimethyl disulfide (DMDS) [8], can be transported into the subsurface region of copper by shear at the interface [9, 10]. Here, the tribological conditions were selected such that the interfacial temperature rise was negligible (<1 K) thereby allowing thermal effects to be excluded. A rationale for these observations comes from molecular dynamics (MD) simulations of sliding interfaces which reveal the development of a Kelvin–Helmholtz instability [11, 12] leading to shear-induced vortices in the surface region that cause surface atoms to be transported into the bulk [13–18]. The MD simulations showed that the width of the deformed zone varied as the square root of the sliding time, characteristic of amorphous materials. However, a more detailed analytical model that assumed a material flow law is described by the Herschel–Bulkley model (where the shear stress $\tau_{xy} = \tau_0 + C \left(\frac{du}{dy} \right)^m$ [19], τ_0 and C are parameters of the model, m is strain-rate sensitivity, which can take values between 0 and 1, and $\frac{du}{dy}$ is the shear strain rate) showed that the time dependence t of the variation in the characteristic width of the deformed zone, y^* depended critically on the value of m [20]. It was predicted that for $m = 1$, $y^* \propto t^{1/2}$ as found in the MD simulations. However, many metals have $m \sim 0$, [21, 22] leading to $y^* \propto t$. Thus, the sliding time dependence of the width of the deformed zone depends in detail on the value of the strain-rate sensitivity, m . It has been found that the strain-rate sensitivity of metals in general, and of copper in particular, often increases with increasing disorder and the

presence of nanocrystallites [21–27]. However, the copper samples used for the tribological experiments have been shown to exhibit a square low-energy electron diffraction pattern [8] and therefore have rather well ordered surfaces. It might be expected, therefore, that initial sliding against copper, when the strain-rate sensitivity is close to zero, would lead to a linear variation of the width of the deformed zone with time.

Continually dosing a copper surface with DMDS while sliding leads to a reduction in friction, consistent with the shear-induced formation of a boundary film [10, 28]. However, it was also found that no reduction in friction was observed for DMDS at higher loads [10]. This is in contrast to what might be expected for a thermally induced boundary film, where higher loads would lead to higher interfacial temperatures and therefore more rapid thermal diffusion into the bulk. In order to attempt to understand this phenomenon in greater detail, and to provide a more robust test of the predictions of the MD simulations and analytical models of shear-induced surface-to-bulk transport, the following explores the kinetics of material transport from the surface into the bulk due to interfacial shear, and the concentration profile of the resulting boundary film.

We note, in this context, that the tribological experiments used to explore shear-induced surface-to-bulk transport involve repeated intermittent sliding as opposed to the MD simulations where the sliding is continuous [13–18]. In the experiment described below in which the surface is continually dosed with DMDS, the surface becomes saturated with an adsorbed overlayer of thiolate species between passes. Thus, for an experiment carried out with a total number of passes n , the overlayer that was formed on the surface during the first pass will have been rubbed n times, whereas the overlayer that forms on the surface during the final pass will only have been rubbed once. This implies that a layer that has been rubbed some intermediate number of times, say p , will have penetrated the sample a distance $\propto p^x$ where, as indicated above, the exponent x will depend on the value of the strain-rate sensitivity, m where x is 0.5 for $m = 1$, and unity for $m = 0$ [20].

These issues are explored using two experimental strategies. In the first, the coverage of an initially saturated methyl thiolate overlayer formed by dosing the copper surface with DMDS at 300 K is monitored as a function of the number of times it had been rubbed. In the second experiment, the depth profile of a boundary film formed by continually dosing a copper surface with DMDS while rubbing is measured.

2 Experimental

Tribological measurements were carried out in a stainless-steel, ultrahigh vacuum (UHV) chamber operating at a base

pressure of $\sim 2 \times 10^{-10}$ Torr following bakeout, which has been described in detail elsewhere [29]. Briefly, the chamber was equipped with a UHV-compatible tribometer, which simultaneously measures normal load, lateral force, and the contact resistance between the tip and substrate. All tribological measurements were made with unidirectional sliding using a speed of ~ 4 mm/s at a normal load of 0.44 N. Previous work has shown that the maximum interfacial temperature rise for a copper sample under these conditions is much less than 1 K [9]. The spherical tribopin (~ 1.27 cm diameter) was made from tungsten carbide containing some cobalt binder and could be heated by electron bombardment in vacuo to clean it. Experiments were performed by initially rubbing the tribopin against the clean copper sample ($\sim 1 \times 1$ cm² by ~ 1 mm thick) until a constant friction coefficient was obtained. This resulted in the formation of a wear track on the surface and likely in the transfer of copper to the tribopin so that friction results are for a sliding copper–copper interface. The DMDS was dosed through a leak valve connected to a dosing tube (with an internal diameter of 4 mm) directed toward the sample so that the pressure at the sample is enhanced compared to the measured background pressure, which was set at 2×10^{-8} Torr during DMDS dosing (where pressures are not corrected for ionization gauge sensitivity). The interval between each scan is ~ 20 s resulting in an unenhanced DMDS exposure of ~ 0.4 L [1 L (Langmuir) = 1×10^{-6} Torr s]. This suggests that the total enhanced exposure between scans is sufficient to saturate the surface with the adsorbed molecule.

The chamber also contained a single-pass, cylindrical-mirror analyzer for Auger analysis, and an argon ion bombardment source for sample cleaning and depth profiling. Auger spectra were collected using an electron beam energy of 5 kV. A high-resolution electron gun with a channeltron secondary electron detector was also incorporated into the system. This allowed scanning electron microscopy images of the wear scar to be collected. Finally, the chamber also included a quadrupole mass spectrometer for leak checking and for gauging reactant purity.

The copper samples (Alfa Aesar, 99.99 % pure, 1 mm thick) were polished to a mirror finish using 1 μ m diamond paste and then rinsed with deionized water and degreased ultrasonically in acetone. Once in UHV, the copper samples were cleaned using a standard procedure which consisted of Argon ion bombardment (~ 1 kV, ~ 2 μ A/cm²) and annealing cycles up to ~ 850 K. The cleanliness of the samples was monitored using Auger spectroscopy.

The DMDS (Aldrich, 99.0 % purity) was transferred to a glass bottle and attached to the gas-handling system of the vacuum chamber, where it was subjected to several freeze–pump–thaw cycles. The purity of the DMDS was monitored using mass spectroscopy.

3 Results

In all experiments, a wear track was initially created by rubbing the clean sample 70 times to ensure that the contact conditions remained the same for subsequent scans. During this process, the friction coefficient dropped from an initial value of ~ 0.8 to a final, constant value of ~ 0.45 [28]. The surface, including the wear track, was then saturated with DMDS at a sample temperature of 300 K to form a methyl thiolate overlayer [8]. An Auger signal profile was obtained while scanning the electron beam across the wear track by monitoring the S KLL Auger signal at 151 eV kinetic energy. The sulfur Auger signal was used in this and subsequent experiments since its cross section is larger than that of carbon. The full Auger spectrum was collected within the wear track and the amount of sulfur on the surface was gauged from the ratio of the peak-to-peak intensities of the S KLL to the Cu LMM Auger features. The surface was then rubbed several times at an applied normal load of 0.44 N and a sliding speed of 4 mm/s. Auger spectra were collected at various sliding intervals until no sulfur was detected on the surface. The resulting plot of the S/Cu Auger ratio as a function of the number of passes is displayed in Fig. 1. The experiment was repeated several times and was very reproducible. The line plotted through the data is a theoretical fit which is described in greater detail in the next section.

A similar experiment was carried out in which an initial wear track was created during a run-in period of 70 scans. The previously rubbed portion of the surface was then rubbed repeatedly at an applied normal load of 0.44 N and a sliding speed of 4 mm/s, while the surface was continuously exposed to gas-phase DMDS from a dosing tube with a background pressure of 2×10^{-8} Torr. After various numbers of passes, an Auger depth profile was obtained by Argon ion bombarding the sample (ion current = $1 \mu\text{A}/\text{cm}^2$, beam energy = 800 eV) [30, 31]. The sulfur Auger signal ratioed to that of copper (S/Cu) for the methyl thiolate overlayer outside the wear track (Fig. 2a, empty square) displays an exponential decrease with ion bombardment time due to sulfur atoms being driven into the substrate as well as being bombarded away. The corresponding S/Cu Auger ratios measured inside the wear scar after various numbers of scans are also shown in Fig. 2a [after 39 (filled square), 130 (filled circle), and 366 (filled triangle) scans]. Note that the S/Cu ratio measured outside the wear track (Fig. 2a, empty square) was identical for all experiments. Thus the initial portion of the depth profile inside the wear track contains contributions both from the sulfur on the surface as well as that which had been transported into the bulk. The surface sulfur Auger signal (at a bombardment time of zero) is larger inside the wear scar than outside, an effect that has been observed

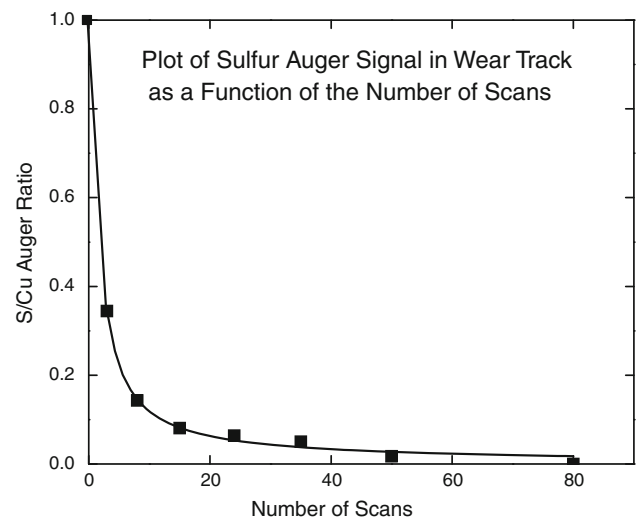


Fig. 1 Plot of the sulfur to copper Auger ratio measured within the wear track for a saturated overlayer of methyl thiolate species on a copper foil as a function of the number of passes of the tribopin with a normal load of 0.44 N at a scanning speed of 4×10^{-3} m/s

previously and ascribed to the rougher surface in the wear track being able to accommodate more thiolate species [28]. Thus, the surface sulfur contribution to the signal is subtracted from the depth profile within the wear track by normalizing the profile outside the track to the S/Cu ratio at the surface to reveal the distribution of subsurface sulfur. This procedure is carried out for surfaces that had been rubbed 39 (filled square), 130 (filled circle), and 366 (filled triangle) times and the results are displayed in Fig. 2b. This demonstrates that sulfur has indeed penetrated the subsurface region, but that the profiles for 130 and 366 scans are almost identical, suggesting that the shear-induced surface-to-bulk transport ceases completely after some number of passes.

4 Analysis of Shear-Induced Surface-to-Bulk Transport Kinetics

In order to analyze the shear-induced sulfur removal results shown in Fig. 1, a model based on the analysis of Karkhikeyan [20] was adopted. The model assumes that shear at the interface causes a layer that has been rubbed some number of times, say p , to penetrate the sample a distance $d \propto p^x$ where the exponent x depends on the value of the strain-rate sensitivity, m . As noted above, when $m = 0$, as typically expected for crystalline metals, $x = 1$, while for $m = 1$, $x = \frac{1}{2}$. We initially analyze this process by assuming that wear is negligible. The initial Auger signal in the data in Fig. 1 (for $p = 0$) is for a methyl thiolate monolayer taken to have some thickness d_0 . Since the depth sensitivity in Auger spectroscopy depends on the electron

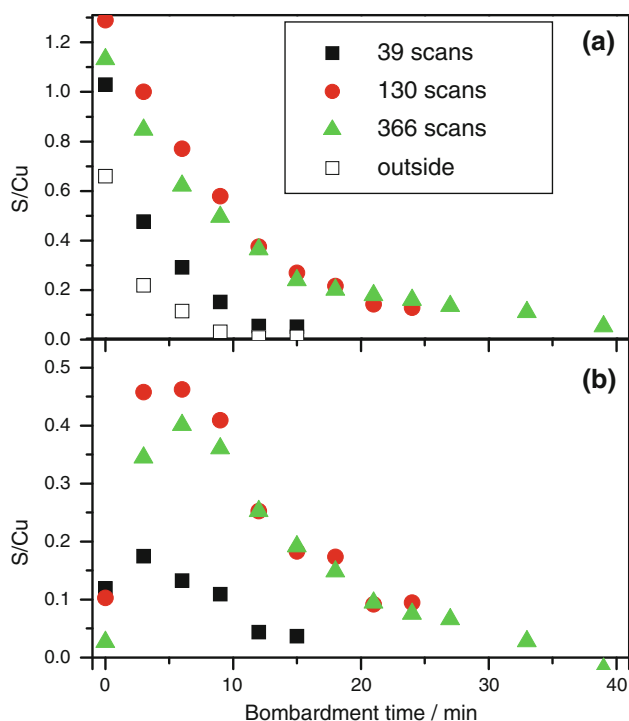


Fig. 2 **a** Sulfur Auger signal depth profile as a function of the Argon ion bombardment time for methyl thiolate species on the surface of a copper foil outside the wear track (*empty square*) and inside the wear track for samples that had been rubbed 39 (*filled square*), 130 (*filled circle*), and 366 (*filled triangle*) times. **b** Shows depth profiles inside the wear track where the surface contribution was subtracted from the profiles in (**a**) for samples that had been rubbed 39 (*filled square*), 130 (*filled circle*), and 366 (*filled triangle*) times. The surface was bombarded with 800 eV Argon ions at a current of 1.0 $\mu\text{A}/\text{cm}^2$

escape depth, z_0 , [32] the measured sulfur intensity for a thiolate monolayer $I(0)$ is given by:

$$I(0) = S \int_0^{d_0} C_0 e^{-z/z_0} dz \quad (1)$$

where S is the Auger sensitivity for sulfur, and C_0 is the monolayer concentration. Integrating Eq. (1) yields $I(0) = SC_0 z_0 (1 - e^{-d_0/z_0})$. If shear causes the sulfur to penetrate a distance d_p during the first pass then the total distance that the layer penetrates after p passes, is $d(p) = d_p p^x$. The initial surface sulfur concentration, taken to be C_0 , must be conserved. If, for simplicity, it is assumed that the sulfur is uniformly distributed throughout the layer of thickness d , then the concentration after p passes can be expressed as $C(p) = C_0/(d_p p^x)$ for a depth $\leq d(p)$, and zero for a depth $> d(p)$. Since the sulfur is assumed to be uniformly distributed, $C(p)$ also gives the sulfur concentration at the surface. In this case, taking account of the Auger depth sensitivity, Eq. (1) becomes:

$$I(p)_{p \geq 1} = SC_0 \left(\frac{d_0}{d_p} \right) \frac{1}{p^x} \int_0^{d_p p^x} e^{-z/z_0} dz \quad (2)$$

This leads to a predicted form of the sulfur Auger signal as a function of the number of passes p as:

$$\frac{I(p)_{p \geq 1}}{I(0)} = \frac{\left(1 - \exp\left(-\left(\frac{d_p}{d_0}\right)\left(\frac{d_0}{z_0}\right)p^x\right)\right)}{\left(p^x\right)\left(d_p/d_0\right)\left(1 - \exp\left(-d_0/z_0\right)\right)} \quad (3)$$

and thus depends on $\frac{d_p}{d_0}$, $\frac{d_0}{z_0}$ and x . $\frac{d_p}{d_0}$ represents the distance that the sulfur has penetrated the substrate relative to the thickness of the initial thiolate layer and $\frac{d_0}{z_0}$ is the thickness of the thiolate layer relative to the electron escape depth. The value of d_0 can be estimated from the atomic radius of sulfur as 0.22 ± 0.02 nm. The electron escape depth at the kinetic energy of the sulfur Auger electrons (at 151 eV), $z_0 \sim 0.6$ nm, [32] yields a value of $\frac{d_0}{z_0} = 0.37 \pm 0.04$ nm. The data in Fig. 1 are, therefore, fit by constraining the value of $\frac{d_0}{z_0}$ to be between 0.2 and 0.5. The line through the experimental data in Fig. 1 shows the fit to Eq. (3), which reproduces the experimental data very well, yielding $x = 0.93 \pm 0.05$ and $\frac{d_p}{d_0} = 3.3 \pm 0.3$. The value of $x \sim 0.93$ is consistent with a strain-rate sensitivity $m = 0$, as expected for sliding on a crystalline metal. It should be noted that Eq. (3) fits the data well even for the largest number (up to 80) of scans with a constant value of x . This implies that, if the value of the strain-rate sensitivity m does vary during rubbing, the change is not sufficient to be detected from the loss of surface species. The good fit also implies that the assumption that the sulfur is uniformly distributed throughout the layer is reasonable. Using the value of d_0 from above yields $d_p = 0.7 \pm 0.1$ nm per scan.

Wear could also occur during sliding. The wear track, once it is formed during the run-in period does not widen significantly so that the subsequent wear is small. Indeed, the amount of material removed per pass must be less than d_0 otherwise all the sulfur would have been worn away during the first pass. If the wear track width varies by only a small amount, a constant wear rate will remove a constant film thickness of w_0 per pass. In this case, the average concentration in the subsurface region remains unaffected since the shear causes the sulfur to be transported to the subsurface. Thus, the total distance that the layer penetrates after p passes is modified to give $d(p) = d_p p^x - p w_0$, and thus affects the upper integration limit in Eq. (2). Evaluating the integral yields a function for $I(p)$ including wear yields

$$\frac{I(p)_{p \geq 1}}{I(0)} = \frac{\left(1 - \exp\left(-\left(\frac{d_p - w_0}{d_0}\right)\left(\frac{d_0}{z_0}\right)p\right)\right)}{p\left(d_p/d_0\right)\left(1 - \exp\left(-d_0/z_0\right)\right)} \quad (4)$$

The fit to the data in Fig. 1 is rather insensitive to $\frac{w_0}{d_0}$ for values ≤ 0.1 and the errors in the other parameters start to increase as $\frac{w_0}{z_0}$ increases above this value; however, the best-fit values only vary very slightly from those produced by the fit to Eq. (3). This indicates that the wear is sufficiently low that it cannot be detected from the data presented in Fig. 1 with the normal load used for this experiment (0.44 N) and is less than ~ 0.06 nm/scan.

Such an analysis enables the sulfur depth profile during continuous rubbing to be explored using a similar model in which the thickness of each shear-induced layer increases by ~ 0.7 nm per pass. If the initial concentration of the sulfur on the surface is again taken to be C_0 , and the total number of passes for the whole experiment is n , then the concentration at some depth in the film z is given by:

$$C(n, z) = C_0 \sum_{p=z/d_p}^n \frac{1}{pd_p}. \tag{5}$$

The sum $H_n = \sum_{p=1}^n \frac{1}{p}$ is the Harmonic number so that:

$$C(n, z) = \frac{C_0}{d_p} \left(H_n - H_{z/d_p} \right). \tag{6}$$

Now $H_n = \ln(n) + \gamma - \frac{1}{2n} - \frac{1}{12n^2} - \frac{1}{120n^5} + O(n^{-6})$ where γ is the Euler–Mascheroni constant. It is sufficient to write the equation to the first order to yield:

$$C(n, z) = \frac{C_0}{d_p} \left(\ln\left(\frac{nd_p}{z}\right) - \frac{1}{2} \left(\frac{1}{n} - \frac{d_p}{z} \right) \right). \tag{7}$$

The calculated concentration depth profile from Eq. (7) is plotted for 39, 130, and 366 scans in Fig. 3. This reveals that the concentration decreases to zero when $\frac{z}{d_p} = n$, where n is the total number of scans. The general concave shapes of the curves are similar to those found experimentally (Fig. 2a). However, as indicated by the depth profile measured for a monolayer of thiolate species outside the wear track (Fig. 2a, empty square), Argon ion bombardment itself causes the sulfur to penetrate the bulk. The effect of sputtering a film of composition $C(z)$ can be gauged by convoluting with a depth resolution function [30, 31], $R(z)$ where the Auger signal at some depth z within the sample, $Y(z)$ is given by:

$$Y(z) = \int_0^z C(z')R(z-z')dz'. \tag{8}$$

The depth profile outside the wear track, due to a monolayer of adsorbed thiolate species (Fig. 2a, empty square), varies exponentially with sputtering time, so that $R(z-z') \sim e^{-\frac{(z-z')}{s_0}}$ and a fit to the curve yields a bombardment decay time of 3.9 min. A removal rate of ~ 3.2 copper atoms per Argon ion has been estimated for

ion bombardment at a beam energy of 1 keV, [33] yielding a value of $s_0 \sim 3$ nm. Performing the convolution of Eq. 7 yields an equation for the predicted Auger depth profile:

$$Y(n, z) = C \frac{s_0}{d_p} \left(\ln\left(\frac{nd_p}{z}\right) + e^{-z/s_0} \left(\ln\left(\frac{z}{nd_p}\right) + \left(\frac{z}{s_0}\right) + \frac{1}{4} \left(\frac{z}{s_0}\right)^2 + \frac{1}{18} \left(\frac{z}{s_0}\right)^3 \right) \right). \tag{9}$$

This depth profile is plotted in Fig. 4 for the simulations shown in Fig. 3, with $s_0 = 3$ nm and $d_p = 0.7$ nm. A similar analysis for a sample with a strain-rate sensitivity of $m = 1$, which would give a depth per pass given by $d(p) = d_p p^{1/2}$ yields an almost linear variation of concentration with depth, $C(n, z)$.

5 Discussion

The kinetics of shear-induced surface-to-bulk transport of a methyl thiolate overlayer formed on a copper surface have been explored. The analysis of the shear-induced removal kinetics of the thiolate overlayer within the wear track (Fig. 1) suggests that the shear front moves a distance that is proportional to the number of scans, by ~ 0.7 nm per scan. It has been previously demonstrated that the sulfur moves to the subsurface region [9], and the linear variation of penetration distance with the number of scans is consistent with the behavior for a metal with a value of strain-rate sensitivity close to zero. Including wear in the analysis

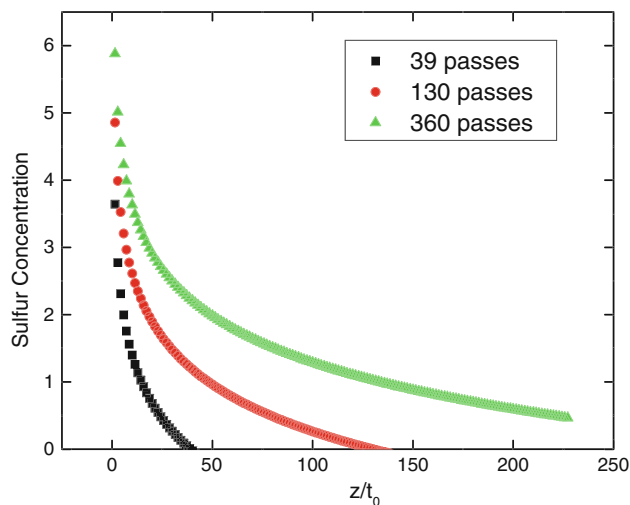


Fig. 3 Simulation of the sulfur concentration variation within the sample for sliding on a copper surface assuming that a uniform front moves proportionately to the number of passes at a distance of 0.7 nm per pass for samples that had been rubbed 39 (filled square), 130 (filled circle), and 366 (filled triangle) times

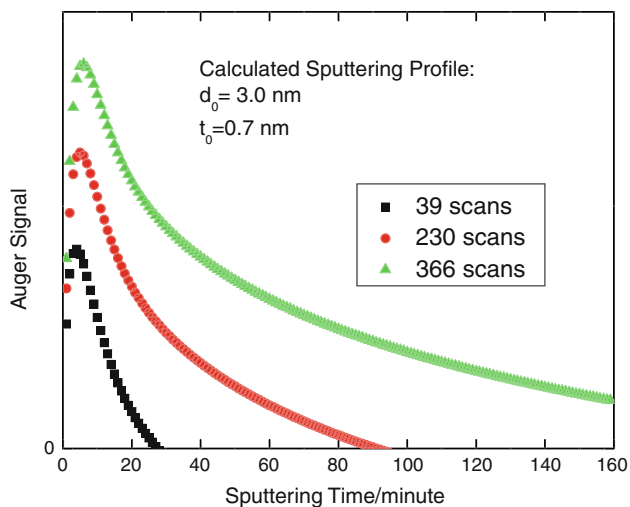


Fig. 4 Simulation of the Argon ion depth profile for the sulfur concentration distributions shown in Fig. 3 for samples that had been rubbed 39 (filled square), 130 (filled circle), and 366 (filled triangle) times

does not change the form of the fit to the data in Fig. 1, suggesting that the wear rate is less than ~ 0.06 nm/scan under an applied load of 0.44 N.

A similar experiment was performed while the sample surface was continually replenished with DMDS to ensure that it was saturated with methyl thiolate species between each scan. The sulfur depth profiles collected following these experiments are displayed in Fig. 2a for measurements within the wear track as a function of ion bombardment time after the sample had been scanned 39, 130, and 366 times. The contribution of the sulfur on the surface was subtracted out (using the shape of the profile for a thiolate overlayer outside the wear track in Fig. 2a, empty square) and the resulting subsurface sulfur distributions are displayed in Fig. 2b. This shows that sulfur has indeed penetrated the subsurface region, but that the depth profile does not change substantially when the number of scans is increased from 130 to 366. It is interesting to note that similar subsurface elemental distributions were found for an oil-lubricated contact where the elements in zinc dialkyl dithiophosphate were found in the subsurface region with similar distributions [34].

In order to establish the form of the depth profile that would be expected for a material with a strain-rate sensitivity of zero, as found from the data shown in Fig. 1, a simple model was adopted in which the front during each pass moves a distance d_p into the sample so that the thiolate species adsorbed during the first pass would penetrate further into the substrate than those at the end of the experiment. This model is certainly consistent with the assumption used to fit the data in Fig. 1. The results of the simulation are shown in Fig. 3, where, as expected, the

concentration decreases to zero, as it should, at a distance $n \times d_p$, where n is the total number of passes. All the curves show the concave behavior seen for the experimental depth profiles (Fig. 2a). Note that, using a similar analysis as carried out in the previous section, a front that moves as \sqrt{n} , as would be expected for strain-rate sensitivity of unity [20], would show an almost linear concentration variation with depth. The simulations show a significant difference in the profiles after 130 and 366 scans, while the measured depth profiles are almost identical. In fact, increasing the number of scans even more (to 500) reveals that, even within the existing model the profile close to the surface starts to change rather slowly. The data shown in Fig. 2a were not rubbed for a sufficient number of times for this to have occurred.

In order to gauge how the depth profile is influenced by the Argon bombardment measurement, the forms of the Auger depth profiles for the model results in Fig. 3 were simulated by convoluting with a depth resolution function obtained for the thiolate overlayer outside the wear track (Fig. 2a, empty square). The results are displayed in Fig. 4 and the general features of the experimental profiles are reproduced quite well; the agreement with the experimental profile after 39 scans is good. The peaks in the profiles arise from the width of the depth resolution function and shift to slightly longer times for profiles collected with increasing number of scans, as found experimentally. However, the simulations for 130 and 366 scans are significantly different from the experiment. In particular, in the experiment, the signal decreases to zero after 40 min of bombardment after scanning 130 and 366 times, while the simulations indicate that it should have persisted for 90 min or more. This suggests that the model proposed above fits well with experiment for an overlayer rubbed a relatively low number (~ 40) of times.

Clearly the nature of the interface is changing as sulfur (and carbon) penetrates the subsurface region and the resulting boundary film causes a decrease in friction coefficient [10, 28]. While the sulfur signal is monitored since it has the largest Auger cross section, carbon is also present in the thiolate layer [28] so that it is clear that the material properties of the surface region will change as its chemical composition changes. This could well affect the value of the strain-rate sensitivity, thereby altering the shear-induced transport kinetics and may also change the value of d_p causing the elemental depth profile to not change at larger numbers of scans. In addition, a relatively large sulfur concentration is found on the surface of the wear scar. The reduction in friction found when copper is lubricated using DMDS indicates a reduction in shear strength, thus forming a friction-reducing surface structure that would inhibit the formation of Kelvin–Helmholtz instabilities by localizing shear, which could also cause the

surface-to-bulk transport to cease. Further work is needed to unequivocally identify the origins of this effect. Nonetheless, the film growth mechanism is self limiting as required for an effective lubricant. As the film is worn from the surface, the shear-induced mechanism will once again operate to replenish the boundary film.

6 Conclusions

The kinetics of shear-induced surface-to-bulk transport of methyl thiolate species formed on a copper surface by exposure to DMDS were explored. In the first type of experiment, the loss of surface species in the wear track was measured as a function of the number of passes by Auger spectroscopy. It is found that the results can be reproduced extremely well using a model in which the adsorbate initially present on the surface moves a distance of ~ 0.7 nm per pass. This is in agreement with a theoretical analysis of the shear-induced Kelvin–Helmholtz instabilities for a material where the shear properties can be described by a strain-rate sensitivity of zero, consistent with a crystalline metal substrate. Adding the effect of wear does not improve the fit to the experimental data and therefore suggests that wear is minimal under the conditions used for the experiment.

The sulfur depth profile is also measured when the surface is continually exposed to DMDS while rubbing. The resulting experimentally measured shape of the depth profile is consistent with the surface-to-bulk transport kinetics found by monitoring the change in adsorbate coverage as a function of the number of scans. However, the depth profiles found after 130 and 366 scans are almost identical indicating that the shear-induced transport of the surface species when using DMDS is self limiting. This effect could be due to either a change in the material properties of the near-surface region that quenches the formation of the Kelvin–Helmholtz instabilities or the formation of a boundary film that localizes the shear.

Acknowledgments We gratefully acknowledge the Chemistry Division of the National Science Foundation under Grant Number CHE-9213988 and the Office of Naval Research for support of this work. We also thank Professor David Rigney for extremely useful discussions and suggestions during the course of this work.

References

- Panin, V., Kolubaev, A., Tarasov, S., Popov, V.: Subsurface layer formation during sliding friction. *Wear* **249**(10–11), 860–867 (2001). doi:[10.1016/s0043-1648\(01\)00819-5](https://doi.org/10.1016/s0043-1648(01)00819-5)
- Tarasov, S., Rubtsov, V., Kolubaev, A.: Subsurface shear instability and nanostructuring of metals in sliding. *Wear* **268**(1–2), 59–66 (2010). doi:[10.1016/j.wear.2009.06.027](https://doi.org/10.1016/j.wear.2009.06.027)
- Moshkovich, A., Perfilyev, V., Lapsker, I., Gorni, D., Rapoport, L.: The effect of grain size on Stribeck curve and microstructure of copper under friction in the steady friction state. *Tribol. Lett.* **42**(1), 89–98 (2011). doi:[10.1007/s11249-011-9752-3](https://doi.org/10.1007/s11249-011-9752-3)
- Moshkovich, A., Perfilyev, V., Lapsker, I., Rapoport, L.: Stribeck curve under friction of copper samples in the steady friction state. *Tribol. Lett.* **37**(3), 645–653 (2010). doi:[10.1007/s11249-009-9562-z](https://doi.org/10.1007/s11249-009-9562-z)
- Mishra, A., Kad, B.K., Gregori, F., Meyers, M.A.: Microstructural evolution in copper subjected to severe plastic deformation: experiments and analysis. *Acta Mater.* **55**(1), 13–28 (2007). doi:[10.1016/j.actamat.2006.07.008](https://doi.org/10.1016/j.actamat.2006.07.008)
- Gubicza, J., Chinh, N.Q., Csanádi, T., Langdon, T.G., Ungár, T.: Microstructure and strength of severely deformed fcc metals. *Mater. Sci. Eng. A* **462**(1–2), 86–90 (2007). doi:[10.1016/j.msea.2006.02.455](https://doi.org/10.1016/j.msea.2006.02.455)
- Zhang, Y.S., Han, Z., Wang, K., Lu, K.: Friction and wear behaviors of nanocrystalline surface layer of pure copper. *Wear* **260**(9–10), 942–948 (2006). doi:[10.1016/j.wear.2005.06.010](https://doi.org/10.1016/j.wear.2005.06.010)
- Furlong, O.J., Miller, B.P., Li, Z., Walker, J., Burkholder, L., Tysoe, W.T.: The surface chemistry of dimethyl disulfide on copper. *Langmuir* **26**(21), 16375–16380 (2010). doi:[10.1021/la101769y](https://doi.org/10.1021/la101769y)
- Furlong, O., Miller, B., Tysoe, W.: Shear-induced surface-to-bulk transport at room temperature in a sliding metal–metal interface. *Tribol. Lett.* **41**(1), 257–261 (2011). doi:[10.1007/s11249-010-9711-4](https://doi.org/10.1007/s11249-010-9711-4)
- Furlong, O., Miller, B., Tysoe, W.T.: Shear-induced boundary film formation from dialkyl sulfides on copper. *Wear* **274–275**, 183–187 (2012). doi:[10.1016/j.wear.2011.08.022](https://doi.org/10.1016/j.wear.2011.08.022)
- Thomson, W.: Hydrokinetic solutions and observations, XLVI. *Philos. Mag. Ser.* **42**(281), 362–377 (1871). doi:[10.1080/14786447108640585](https://doi.org/10.1080/14786447108640585)
- Helmholtz, H.V.: Über discontinuierliche Flüssigkeits-Bewegungen. *Monatsberichte der Königlichen Preussische Akademie der Wissenschaften zu Berlin*, vol 23, p. 13 (1868)
- Kim, H.J., Kim, W.K., Falk, M.L., Rigney, D.A.: MD simulations of microstructure evolution during high-velocity sliding between crystalline materials. *Tribol. Lett.* **28**(3), 299–306 (2007). doi:[10.1007/s11249-007-9273-2](https://doi.org/10.1007/s11249-007-9273-2)
- Emge, A., Karthikeyan, S., Kim, H.J., Rigney, D.A.: The effect of sliding velocity on the tribological behavior of copper. *Wear* **263**, 614–618 (2007). doi:[10.1016/j.wear.2007.01.095](https://doi.org/10.1016/j.wear.2007.01.095)
- Kim, H.J., Karthikeyan, S., Rigney, D.: A simulation study of the mixing, atomic flow and velocity profiles of crystalline materials during sliding. *Wear* **267**(5–8), 1130–1136 (2009). doi:[10.1016/j.wear.2009.01.030](https://doi.org/10.1016/j.wear.2009.01.030)
- Karthikeyan, S., Agrawal, A., Rigney, D.A.: Molecular dynamics simulations of sliding in an Fe–Cu tribopair system. *Wear* **267**(5–8), 1166–1176 (2009). doi:[10.1016/j.wear.2009.01.032](https://doi.org/10.1016/j.wear.2009.01.032)
- Emge, A., Karthikeyan, S., Rigney, D.A.: The effects of sliding velocity and sliding time on nanocrystalline tribolayer development and properties in copper. *Wear* **267**(1–4), 562–567 (2009). doi:[10.1016/j.wear.2008.12.102](https://doi.org/10.1016/j.wear.2008.12.102)
- Rigney, D.A., Karthikeyan, S.: The evolution of tribomaterial during sliding: a brief introduction. *Tribol. Lett.* **39**(1), 3–7 (2010). doi:[10.1007/s11249-009-9498-3](https://doi.org/10.1007/s11249-009-9498-3)
- Herschel, W., Bulkley, R.: Konsistenzmessungen von Gummi-Benzollösungen. *Colloid Polym. Sci.* **39**(4), 291–300 (1926). doi:[10.1007/bf01432034](https://doi.org/10.1007/bf01432034)
- Karthikeyan, S., Kim, H.J., Rigney, D.A.: Velocity and strain-rate profiles in materials subjected to unlubricated sliding. *Phys. Rev. Lett.* **95**(10), 106001 (2005)
- Zhu, T., Li, J., Samanta, A., Kim, H.G., Suresh, S.: Interfacial plasticity governs strain rate sensitivity and ductility in

- nanostructured metals. *Proc. Nat. Acad. Sci.* **104**(9), 3031–3036 (2007). doi:[10.1073/pnas.0611097104](https://doi.org/10.1073/pnas.0611097104)
22. Shen, Y.F., Lu, L., Dao, M., Suresh, S.: Strain rate sensitivity of Cu with nanoscale twins. *Scr. Mater.* **55**(4), 319–322 (2006). doi:[10.1016/j.scriptamat.2006.04.046](https://doi.org/10.1016/j.scriptamat.2006.04.046)
 23. Mishra, A., Martin, M., Thadhani, N.N., Kad, B.K., Kenik, E.A., Meyers, M.A.: High-strain-rate response of ultra-fine-grained copper. *Acta Mater.* **56**(12), 2770–2783 (2008). doi:[10.1016/j.actamat.2008.02.023](https://doi.org/10.1016/j.actamat.2008.02.023)
 24. Meyers, M.A., Mishra, A., Benson, D.J.: Mechanical properties of nanocrystalline materials. *Prog. Mater. Sci.* **51**(4), 427–556 (2006). doi:[10.1016/j.pmatsci.2005.08.003](https://doi.org/10.1016/j.pmatsci.2005.08.003)
 25. Schwaiger, R., Moser, B., Dao, M., Chollacoop, N., Suresh, S.: Some critical experiments on the strain-rate sensitivity of nanocrystalline nickel. *Acta Mater.* **51**(17), 5159–5172 (2003). doi:[10.1016/s1359-6454\(03\)00365-3](https://doi.org/10.1016/s1359-6454(03)00365-3)
 26. Höppel, H.W., May, J., Göken, M.: Enhanced strength and ductility in ultrafine-grained aluminium produced by accumulative roll bonding. *Adv. Eng. Mater.* **6**(9), 781–784 (2004). doi:[10.1002/adem.200306582](https://doi.org/10.1002/adem.200306582)
 27. Gray Iii, G.T., Lowe, T.C., Cady, C.M., Valiev, R.Z., Aleksandrov, I.V.: Influence of strain rate & temperature on the mechanical response of ultrafine-grained Cu, Ni, and Al–4Cu–0.5Zr. *Nanostruct. Mater.* **9**(1–8), 477–480 (1997). doi:[10.1016/s0965-9773\(97\)00104-9](https://doi.org/10.1016/s0965-9773(97)00104-9)
 28. Furlong, O.J., Miller, B.P., Kotvis, P., Tysoe, W.T.: Low-temperature, shear-induced tribofilm formation from dimethyl disulfide on copper. *ACS Appl. Mater. Interfaces* **3**(3), 795–800 (2011). doi:[10.1021/am101149p](https://doi.org/10.1021/am101149p)
 29. Gao, F., Furlong, O., Kotvis, P.V., Tysoe, W.T.: Pressure dependence of shear strengths of thin films on metal surfaces measured in ultrahigh vacuum. *Tribol. Lett.* **31**(2), 99–106 (2008). doi:[10.1007/s11249-008-9342-1](https://doi.org/10.1007/s11249-008-9342-1)
 30. Hofmann, S., Erlewein, J., Zalar, A.: Depth resolution and surface roughness effects in sputter profiling of NiCr multilayer sandwich samples using Auger electron spectroscopy. *Thin Solid Films* **43**(3), 275–283 (1977). doi:[10.1016/0040-6090\(77\)90289-9](https://doi.org/10.1016/0040-6090(77)90289-9)
 31. Hofmann, S.: Quantitative depth profiling in surface analysis: a review. *Surf. Interface Anal.* **2**(4), 148–160 (1980). doi:[10.1002/sia.740020406](https://doi.org/10.1002/sia.740020406)
 32. Klasson, M., Hedman, J., Berndtsson, A., Nilsson, R., Nordling, C., Melnik, P.: Escape depths of X-ray excited electrons. *Phys. Scr.* **5**(1–2), 93 (1972)
 33. Steinbruchel, C.: Universal energy dependence of physical and ion-enhanced chemical etch yields at low ion energy. *Appl. Phys. Lett.* **55**(19), 1960–1962 (1989)
 34. Dienwiebel, M., Pöhlmann, K.: Nanoscale evolution of sliding metal surfaces during running-in. *Tribol. Lett.* **27**(3), 255–260 (2007). doi:[10.1007/s11249-007-9216-y](https://doi.org/10.1007/s11249-007-9216-y)